



A MAXIMUM POWER POINT TRACKING SCHEME FOR A 1kW STAND-ALONE SOLAR ENERGY BASED POWER SUPPLY

D. B. Nnadi^{1,*}, C. I. Odeh² and C. O. Omeje³

^{1,2}DEPARTMENT OF ELECTRICAL ENGINEERING, UNIVERSITY OF NIGERIA, NSUKKA, ENUGU STATE, NIGERIA

³DEPARTMENT OF ELECTRICAL ENGINEERING, UNIVERSITY OF PORT HARCOURT, RIVERS STATE, NIGERIA

E-mail address: ¹damian.nnadi@unn.edu.ng, ²charles.odeh@unn.edu.ng, ³crescent.omeje@uniport.edu.ng

ABSTRACT

This paper elucidates one of the tracking schemes for a photovoltaic (PV) systems using Cuk converter operating in discontinuous inductor current mode (DICM) as an interface. A method for efficiently maximizing the output power of a solar panel supplying a load or battery bus under varying meteorological conditions is investigated and results presented therein. The incremental conductance (InCond) method of maximum power point tracking (MPPT) using the Cuk's dc to dc converter operating in a discontinuous inductor current mode (DICM) was modeled and studied in relation to PV system interface. Also, laboratory setup was implemented based on the model. This was the main objective of the research. Similarly, the PV simulator was also modeled alongside with Cuk converter operating in DICM. MATLAB/SIMULINK software was used to carry out simulation test. With the incremental conductance method, the problem of sustained oscillation around the maximum power point of the solar panel which is the usual characteristic of the perturbation and observation method is essentially absent. The result disclosed that the power available for the load when MPPT was applied was 1.1 kW which gives a tolerance of 0.1% to the load it powers. But without MPPT, the available power is 0.9 kW using the same number of PV panels and batteries as back up. Hence, MPPT has 17.65% edge in power delivery over non-MPPT PV powered energy supply. An experimental prototype of a 1kW, 230V, 50Hz stand-alone solar based power supply with the incremental conductance scheme was successfully implemented using PIC 16F877 microcontroller, tested and results presented therein. The experimental results agreed with the simulated results.

Keywords: Maximum Power point tracking, Cuk converter, Photovoltaic system, PIC 16F877A micro-controller, inverter, batteries.

1. INTRODUCTION

Energy demand in the pre-industrial world was provided mostly by man and animal power and to a limited extent from the burning of wood for heating, cooking and smelting of metals. The discovery of abundant coal, and the concurrent technological advances and its use, propelled the industrial revolution. Steam engines, mechanized production and improved transportation, all fuelled directly by coal, rapidly followed [1]. But for so many years, the world energy sources depend on conventional sources such as fossil fuel, hydro, coal, radioactive decay, etc. But all these have their peculiar problems of scarcity, rapidly depleting, causing pollution, greenhouse effect and harmful to both man and other living organisms in the environment. Global climate change is a change in the long-term weather patterns [2], in view of this, the Intergovernmental Panel on Climate reported that by the year 2050 earth surface's temperature will rise by 28 °C while the amount of CO₂

emissions must have reduced by 85% [3]. This could occur due to a significant change in the number of natural climate events or, as well, by a number of human-induced climate events. The increased awareness of the environmental impact, the carbon trail of all energy sources, and electric power production, have given stimulus to the growth and adopting of renewable as an alternative energy. Of which solar might cost more than its counterpart renewable energy sources (RES) but is preferred more than others due its abundant in nature. RES such as solar, wind, and tidal were considered as the solution to the aforementioned problems. For the fact that renewable energy sources are clean, pollution-free, harmless, recyclable, distributed throughout the earth and inexhaustible that makes it a better substitute. Moreover, global climatic change, world-wide increase in energy demand, uncertainty in price and availability of non-renewable energy and world energy policies on using environmental friendly source

* Corresponding author, tel : + 234 – 806 – 933 – 5370

of energy have made PV systems suitable for energy generation in recent time. Consequently, the feed-in tariffs policies adopted by many countries, especially in Europe, have supported the spread of photovoltaic (PV) energy resources. Although, PV cells still show some technological limitations in terms of efficiency in power output, thus more research work requiring significant improvements in the exploitation of PV systems were still going on [4].

Nigeria is not left out in such policy, by signing the Electricity Power Reform Act into law in 2005, provided impetus for long term investment and turn-around in the electricity sector, with improved generation and stable power supply delivery. A significant component of the law is the provision made for investment in renewable energy and in off-grid electricity generation to boost rural access to electricity and meet the needs of about 70% of the country's rural communities. But unfortunately, the policy did not see the light of the day. But even as at that, many private sectors and individuals have embarked upon stand-alone PV power as a remedy for frequent power failures in Nigeria.

PV cells exhibit nonlinear characteristics and also have very low energy efficiency, to this effect, in the literature some techniques to extract maximum power from the knee point of PV system under variable atmospheric conditions have been developed. Maximum power point tracking (MPPT) scheme is used to extract maximum power from PV systems. Various types of MPPT schemes have been developed in literature: The perturbation and observation (P&O) algorithm or Hill-climb Search Method (HCS) [5 -7] is one of the simplest MPPT methods of extracting or tracking power from PV systems. More so, Sofia Lalouni et al. [8] extend the same method to apply to wind energy conversion. Others include voltage and current based MPPT method [9], fractional open-circuit voltage [10], fuzzy logic method [11], etc. have been proffered. Similarly, a subpanel MPPT converter (SPMC), according to Wang et al [12]. was proffered to better address the real-world mismatch issues in MPPT of PV systems. The SPMC system with a unified output MPPT control structure reduces the cost and simplifies the distributed MPPT system. Since the inception of microcontrollers and digital signal processors (DSPs), that have given researchers the enablement to alter the control algorithm without serious modifications of the system hardware platform, digital implementations of MPPT have gained popularity due to their wide selection and technological advances. All these advantages have encouraged researches not only in digital controllers in general applications [13], but also in areas of energy sustainability such as solar power [14-16]; more so in wind energy application

[17]. In this regard, [18], did an evaluation of different MPPT topologies of which one is incremental conductance method. A simple PI controller to improve the incremental conductance method, minimizing the error between the actual conductance and the incremental conductance was used by the authors, because the compensator can be adjusted and updated according to the system necessity were the arguments for using PI controller. Although, the evaluation was just theoretical and simulation based, there was no experimental back up. In [19], the authors applied what they called direct control method to incremental conductance method of MPPT. The PI control loop of reference [18] was eliminated, and the duty cycle was adjusted directly in the algorithm. The control loop was simplified, and the computational time for tuning controller gains was eliminated. To compensate the lack of PI controller in the proposed system, a small marginal error of 0.002 was allowed. The paper used Cuk converter as an interface but instead of Cuk operating in DCM, they used Cuk in continuous current mode (CCM). However, in this research work a PIC16F877 microcontroller was used to extract maximum power point from PV system applying a PWM dc - dc Cuk converter operating in discontinuous inductor current mode to match with the output resistance of the panel as interface. None of the papers reviewed has ever used Cuk in DICM as interface. To avoid much lose in the system as may be incurred in [18], the duty cycle was adjusted directly in the algorithm.

In practice, there are three possible approaches for maximizing the solar power extraction in medium- and large-scale systems. They are sun tracking, maximum power point tracking (MPPT) or both [20]. For small-scale systems, MPPT is popular for economic reasons.

The main focus of this research is to efficiently extract and maximize the output power of a solar panel supplying a load or battery bus under varying meteorological conditions. The proposed MPPT was achieved by connecting a pulse-width-modulated (PWM) dc/dc Cuk converter between a solar panel and a load or battery bus. The converter operates in discontinuous inductor current mode (DICM) which is the interface between the PV systems and the load as seen in Figure 1.

2. METHODOLOGY

Various aspects of the research were modeled in this subheading.

2.1 PV Modeling

Basically, solar cell behaves in the same way as a p-n junction diode. During the dark hours, solar cell is not an active device; it works as a p-n junction. It produces

neither a current nor voltage. However, if connected to an external supply (large voltage), it generates a current I_D , called diode current or dark current. When exposed to the light energy, a DC current is generated. But the generated current (I_{ph}) varies linearly with the solar insolation.

The accuracy, sophistication and complexity of the PV model of Figure 2 can be increased by adding the following in turn:

- Diode saturation current (I_o) which is temperature dependence
- The photo current (I_L) also is temperature dependence
- Series resistance R_s , which gives a more accurate shape between the maximum power point and the open circuit voltage.
- Resistance R_{sh} in parallel with the diode.
- Either introducing two parallel diodes (one with $A = 1$, other with $A = 2$) with independently set saturation currents or allowing the diode quality factor (n) to become a variable parameter (instead of being fixed at either 1 or 2).

Shockley diode is expressed in equation (1) as enumerated by Masters [21],

$$I_D = I_o \left[\exp \left(\frac{q(V + IR_s)}{nkT_c} \right) \right] \quad (1)$$

The solar cell output (I_{sh}) of Figure 2 becomes;

$$I_{sh} = \frac{q(V + IR_s)}{R_{sh}} \quad (2)$$

The output current (I) is given in equation (3)

$$I = I_{ph} - I_D - I_{sh} \quad (3)$$

Substituting equations (1) and (2) into (3), gives equation (4)

$$I = I_{ph} - I_o \left[\exp \left(\frac{q(V + IR_s)}{nkT} \right) \right] - \frac{q(V + IR_s)}{R_{sh}} \quad (4)$$

The output current (I) is given by equation (5),

$$I = I_{sc} - I_d \quad (5)$$

Similarly, the diode current (I_d) is as shown in equation (5),

$$I_d = I_o \left(e^{\frac{V_d}{kT}} - 1 \right) \quad (6)$$

Replacing I_d of the equation (5) by the equation (6) gives the current-voltage relationship of the PV cell as in equation (7). Note equations (1) and (6) are the same except that equation (1) involved R_s and R_{sh} .

$$I = I_L - I_o \left(e^{\frac{V_d}{kT}} - 1 \right) \quad (7)$$

The relationship between the photo-current and temperature is linear (8) and is deduced by noting the change of photo-current with the change of temperature (10).

$$I_L = I_{L(T_1)}(1 + K_o(T - T_1)) \quad (8)$$

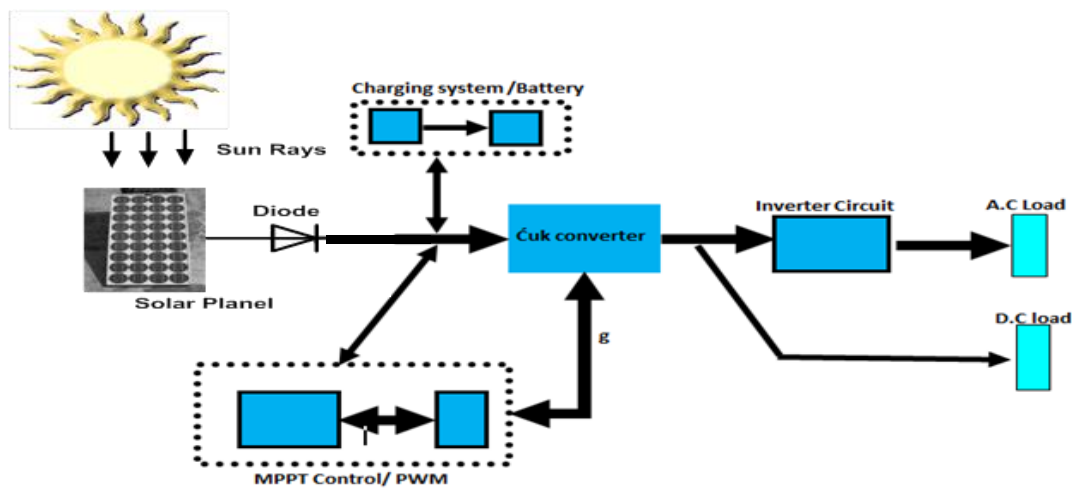


Figure 1: PV Stand-Alone Energy Generation

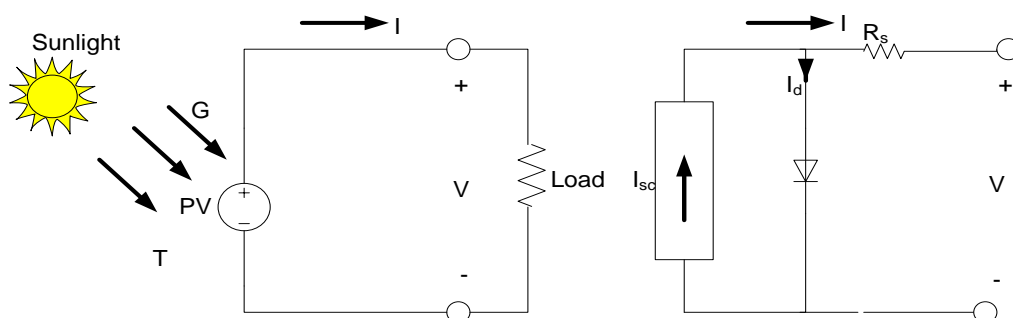


Figure 2: PV cell with a load and its simple equivalent circuit [20]

The photo-current $I_L = I_{ph}$ (A) is directly proportional to irradiance G (Wm^{-2}) when the cell is short circuited, negligible current flows in the diode. Hence, the proportionality constant in equation (9) is set so that the rated short circuit current I_{sc} is delivered under rated irradiance usually $1kWm^{-2}$ at temperature T_1°

$$I_L(T_1) = \frac{G}{G_{nom}} I_{sc}(T_1) \tag{9}$$

K_o is the cell's short-circuit current temperature coefficient is given by;

$$K_o = \frac{(I_{sc}(T_2) - I_{sc}(T_1))}{(T_2 - T_1)} \tag{10}$$

Thus, if the value, I_{sc} , is known from the datasheet, under the standard test condition, $G_{nom}=1000W/m^2$ at the air mass (AM) = 1.5. The reverse saturation current of diode (I_o) is constant under constant temperature and is given by (11).

$$I_o = I_{o(T_1)} * \left(\frac{T}{T_1}\right)^{3/n_s} e^{-qE_g/nk * (\frac{1}{T} - \frac{1}{T_1})} \tag{11}$$

Making the reverse saturation current of diode under reference temperature ($I_{o(T_1)}$) the subject gives equation (12).

$$I_{o(T_1)} = \frac{I_{sc}(T_1)}{(e^{qV_{oc}/nTk} - 1)} \tag{12}$$

where E_g is the band gap voltage = 1.12eV
 This theoretical model gave birth to PV simulator which was modeled in MATLAB/SIMULINK software. The PV simulator was used to power the modeled Cuk converter operating in DIC mode. Simulations were carried out to investigate the effect of varying different meteorological conditions and results obtained.

2.2. Analysis of Cuk Converter Circuit used in the Prototype

A dc-dc converter act as an interface between the load and the PV module whereas the maximum Power point of the PV system was tracked by adjusting the duty cycle of the converter. There are two different conduction modes obtainable in all the dc-dc converters- continuous

conduction mode (CCM) and discontinuous conduction mode (DCM). Modeling the converter will aid in the tracking mechanism since the converter acts as an interface, there is the need to know the relationship between PV system and DC/DC converter.

Discontinuous conduction mode (DCM) occurs in converters because of switching ripple in inductor current or capacitor voltage causing polarity of applied switch current or voltage to reverse, such that the current- or voltage-unidirectional assumptions made in realizing the switch are violated. DCM occurs in dc-dc converter operating at light load (small load current). Sometimes, dc- dc converters and rectifiers are purposely designed to operate in DCM at all loads. To this effect, the properties of converters change radically when DCM is entered:

- DC conversion ratio M becomes load-dependent
- Output impedance is increased
- Dynamics are altered
- Control of output voltage may be lost when load is removed

Cuk converter as a modified buck-boost converter is the first member in the family of three converters that combine the use of inductor and capacitor (instead of only the inductor as described in buck, boost and buck-boost converters) to store energy and sustain the transfer of energy to the converter load. Cuk converter provides capacitive isolation which protects the system against switch failure (unlike the buck topology) [22].The input current of the Cuk and single ended primary inductance converter (SEPIC) topologies is continuous, and they can draw a ripple free current from a PV array that is important for efficient MPPT. Figure 3 shows the Cuk'sup-down converter circuit configuration having two filter inductances L_1 and L_2 and an energy transfer capacitor C_m . In analyzing circuit configuration above, it is observed that the current that flows out of node 3 when the switch is closed is the sum of the two inductor currents i_{L1} and i_{L2} .

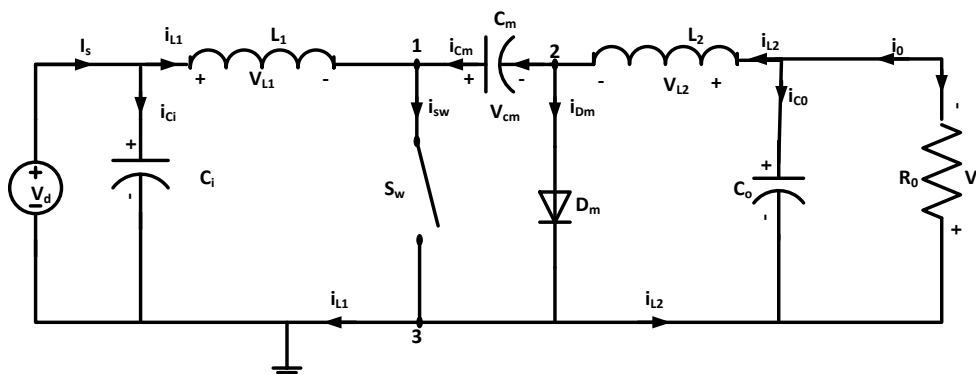


Figure 3:Cuk converter topology

The unregulated dc input voltage V_s can be regulated to dc output voltage V_o by variation of the duty cycle (D). It is assumed that the input and the output filter capacitors C_i and C_o are large enough to make the input voltage and current (V_o, I_o) ripple content negligible. The equivalent circuit of solar array connecting to a maximum power point tracker (MPPT) is shown in Figure 4. The solar array is modeled using a Thevenin's equivalent circuit [23- 24], which consists of a voltage source (V_g) connected in series with an output resistance (r_g) around the MPP. Both v_g and r_g are subject to the level of insolation and temperature. The input voltage and equivalent input resistance of the converter are v_i and r_i respectively. Assuming that there is no converter loss i.e. a lossless condition, the input power P_i going into the tracker is equal to the output power P_o of the solar array. Hence,

Input power P_i = output power P_o

$$P_i = P_o = \frac{v_i^2}{r_i} \tag{13}$$

The rate of change of P_i with respect to v_i and r_i has been expressed in Equation (14)

$$\partial P_i = 2 \frac{v_i}{r_i} \partial v_i + \frac{d(v_i^2)}{\partial r_i^2} = 2 \frac{v_i}{r_i} \partial v_i - \frac{v_i^2}{r_i^2} = \partial r_i \tag{14}$$

For maximum power transfer, this condition holds $r_i=r_g$

$$dP_i = 0, \quad 2 \frac{v_i \delta v_i}{r_i} = \frac{V_i^2}{r_i^2} \delta r_i, \quad \delta v_i = \frac{V_i}{2r_i} \delta r_i \tag{15}$$

If the variation in v_i is small about the average input voltage value V_i , bearing in mind that at MPP the rate of change of P equals zero and r_i equals r_g ; then the above equation can be written as;

$$dv_i = \frac{V_i}{2r_i} dr_i, (r_i \approx r_g) \tag{16}$$

where V_i is the average input voltage. Then, equation (16) gives the required dynamic input characteristic of the tracker at the MPP when v_i has small signal variation of δv_i , subject to a small signal change of δr_i .

In Figure 4, the converter that connects to the solar panel is a Cuk converter operating in discontinuous inductor current mode (DICM) or discontinuous capacitor voltage mode (DCVM) [25- 26] which are two forms of DCM. In DCM three stage are passed before the cycle is completed, the first stage is at the interval $0 \leq t \leq dT_s$, the switch (S_w) is closed, while diode (D_m) is open and d is the duty cycle, also the capacitor voltages are constant throughout a switching period T_s but the output inductor current is negative at the beginning of the state S_w being ON, D_m OFF of DCM.

In discontinuous current conduction mode of Figure 5, the inductor currents, (i_{L1} and i_{L2}) in the interval $0 \leq t \leq DT$ increase linearly from equal magnitudes but opposite in sign $I_{L11} = -I_{L21} = I_{Lx1}$, at $t = 0$ to

I_{L21} and I_{L22} respectively at $t = DT$; where I_{L11}, I_{L21} etc. are the integration constants and can be determined by evaluating equations at the value of $t = 0, DT, t_x, T$ respectively and the corresponding value of the inductor current i.e., $i_{L1} = i_{L1min}$ and so on. With S_m turned off at $t = DT$, the resultant linearly decreasing current sum is now forced to flow through D_m till time $t = t_x$ when the diode current becomes zero thus causing D_m to be off for the rest of the switching cycle. In this interval ($t_x \leq t \leq T$), D_m is off then the inductor currents assume non-time varying values (I_{L11} which is positive and $I_{L21} = -I_{L11}$ which is negative) which forces the inductor voltages to collapse to zero.

$$i_{L1} = -i_{L2} = I_{L11}, \quad t_x \leq t \leq T \tag{17}$$

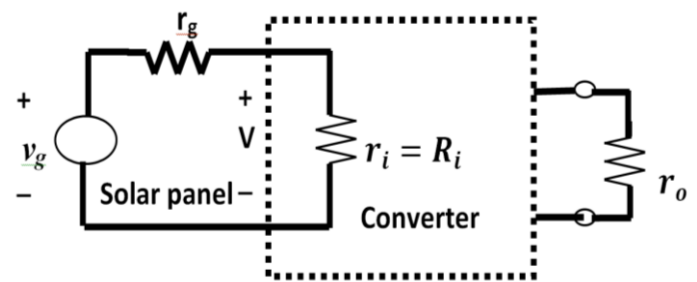


Figure 4: Thevenin's equivalent of a solar panel connecting to a converter [25-26]

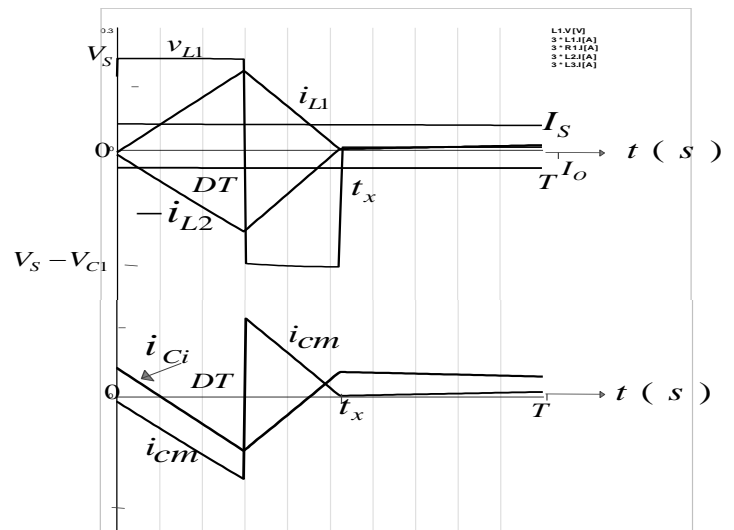


Figure 5: Different waveforms in Cuk DCM.

$$I_{L1} = I_{L2} = 0 \quad t_x \leq t \leq T \tag{18}$$

Essentially, therefore, discontinuous current conduction is the case if the main diode current at $t = T$ is less than zero while continuous load current conduction is the case otherwise. For discontinuous current conduction, therefore, the following relation obtains.

$$I_{L11} + I_{L21} < 0 \tag{19}$$

That is

$$-\frac{I_o}{1-D} + \frac{V_o(1-D)}{2f} \left(\frac{1}{L_{m1}} + \frac{1}{L_{m2}} \right) < 0 \quad (20)$$

That is

$$\frac{(1-D)^2 R}{2fL_r} < 1 \quad (21)$$

Where

$$\frac{1}{L_r} = \frac{1}{L_{m1}} + \frac{1}{L_{m2}}$$

The relation between V_s, V_{cm} and V_o in a cycle of operation is easily determined in the interval $t_x \leq t \leq T$ as

$$V_s = V_{cm} + V_o \quad (22)$$

From the waveforms of I_{L1} and I_{L2} in Figure 5, the voltages V_{cm} and V_o can be shown to be given by

$$\frac{V_{cm}}{V_s} = \frac{t_x/T}{t_x/T - D} \quad (23)$$

$$\frac{V_o}{V_s} = \frac{-D}{t_x/T - D} \quad (24)$$

The changes ($\Delta i_{LM1}, \Delta i_{LM2}$) in inductors L_{M1} , and L_{M2} currents (i_{LM1}, i_{LM2}) are

$$\Delta i_{LM1} = I_{L12} - I_{L11} = \frac{V_s D}{fL_{m1}} \quad (25)$$

$$\begin{aligned} \Delta i_{LM2} &= I_{L12} - I_{L21} = I_{L22} + I_{L11} = \frac{(V_o + V_{cm})D}{fL_{m2}} \\ &= \frac{V_s D}{fL_{m2}} \end{aligned} \quad (26)$$

The averages of inductors I_{m1} and I_{m2} currents (i_{LM1}, i_{LM2}) are respectively I_s and I_o

$$\begin{aligned} I_s &= \frac{1}{T} \int_0^T i_{LM1} dt = I_{L11} + \frac{t_x}{2T} (I_{L12} - I_{L11}) \\ &= I_{L11} + \frac{t_x}{2T} \left(\frac{V_s D}{fL_{m1}} \right) \end{aligned} \quad (27)$$

$$\begin{aligned} -I_o &= \frac{1}{T} \int_0^T i_{LM2} dt = I_{L21} + \frac{t_x}{2T} (I_{L22} - I_{L21}) \\ &= -I_{L21} + \frac{t_x}{2T} (I_{L22} + I_{L11}) \\ &= -I_{L11} + \frac{t_x}{2T} \left(\frac{V_s D}{fL_{m2}} \right) \end{aligned} \quad (28)$$

Adding equations (27) and (28), the result is

$$I_s - I_o = \frac{V_s D t_x}{2} \left(\frac{1}{L_{m2}} + \frac{1}{L_{m1}} \right) = \frac{V_s D t_x}{2L_T} \quad (29)$$

$$\text{where } \frac{1}{L_{m1}} + \frac{1}{L_{m2}} = \frac{V_s D t_x}{L_T} \quad (30)$$

$$\text{when } I_s = \frac{I_o V_o}{V_s} \text{ and } t_x = \frac{DT(V_s - V_o)}{V_o}$$

Obtained from equations (24) through (28) is substituted into equation (29), the result is

$$V_o = -V_s D \sqrt{\frac{R}{2fL_T}} \quad (31)$$

2.3 Determination of Inductors Size

The inductors size is decided such that the change in inductor currents is no more than 5% of the average

inductor current. The following equation gives the change in inductor current [25]

$$\Delta i_L = \frac{V_s D}{L \cdot f_{sw}} \quad (32)$$

where: V_s is the input voltage, D is the duty cycle, and f is the switching frequency. Solving this for L gives:

$$L = \frac{V_s \cdot D}{\Delta i_L \cdot f_{sw}} \quad (33)$$

$$\text{but from } P_o = I_o V_o \quad (34)$$

$$\therefore I_o = \frac{P_o}{V_o} = \frac{145}{14.5} = 10A$$

Assume that the worst current ripple will occur under the maximum power condition. Under this condition, the average current (I_{L1}) of the input inductor (L_i) is 10A, and the ripple current is 5% of I_{L1} .

$$\Delta i_{L1} = 0.05 * I_{L1} = 0.05 * 10 = 0.5A$$

For discontinuous current conduction, this condition must be fulfilled.

$$I_{L1} + I_{L2} < 0 \quad (35)$$

That is

$$-\frac{I_o}{1-D} + \frac{V_o(1-D)}{2f} \left(\frac{1}{L_{m1}} + \frac{1}{L_{m2}} \right) < 0 \quad (36)$$

Hence

$$\frac{1 - D^2 R}{2fL_r} < 1 \quad (37)$$

$$\text{where } \frac{1}{L_r} = \frac{1}{L_{m1}} + \frac{1}{L_{m2}}$$

From equation (37)

$$\frac{2}{L_{mc}} = \frac{2f}{(1-0.8)^2 R} \quad (38)$$

For the duty cycle of the range of 40% to 80% has L_{mc} of 155.5µH to 17.5µH

Applying equation test for load current operating in discontinuous mode which says that if I_{min} of the converter is less than zero the load current is in discontinuous mode. The equation is;

$$I_{min} = \frac{V_s}{R} \left[\frac{1 - e^{-\frac{t_{on}}{\tau}}}{1 - e^{-\frac{T}{\tau}}} \right] - \frac{E}{R} \quad (39)$$

In (39), t_{on} is period at which the switch is ON, E is the load voltage and R is the resistance in ohms. Solving using the range gave I_{min} less than zero shows that the converter is operating in discontinuous mode.

Any value of inductor chosen within the range will make the Cuk converter to operate in discontinuous mode with the range of 0.4 - 0.8 duty cycles. The values for two inductors L_{m1} & L_{m2} are the same in this case 92µH each is used. From the analysis, it is observed that the inductors L_{m1} and L_{m2} , the duty cycle D and the switching frequency affects the converter mode of operation. The Figure 6 shows inductor current in discontinuous mode, the charging and discharging waveform, while Figure 7 shows the laboratory realization of inductor currents in discontinuous mode.

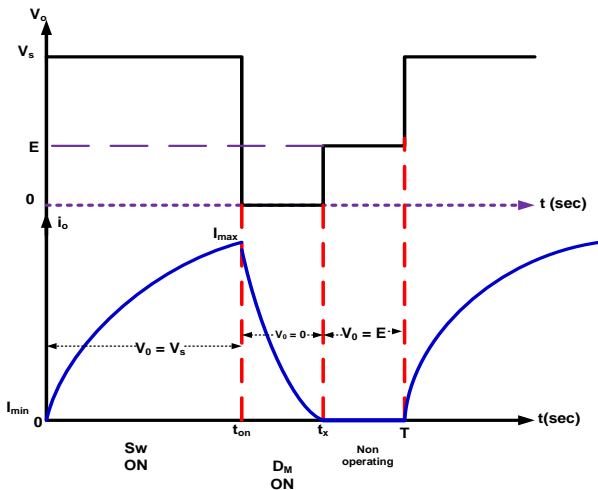


Figure 6: Discontinuous load current mode

2.4 Capacitor Selection

The design criterion for capacitor is that the ripple voltage across it should be less than 5%. Therefore, the average voltage across the capacitor (C_1), going by this equation; $V_{c1} = V_s + V_o$, where $V_s = 16.2$ V and $V_o = 14.5$ V gives;

$$V_{c1} = 16.2 + 14.5 = 30.7V,$$

So, the maximum ripple voltage which is less than 5% of V_{c1} is given by

$$\Delta V_{C1} = 0.05 \times 30.7 = 1.534V.$$

The equivalent load resistance (where the load is battery) is:

$$R = \frac{V_o^2}{P_o} = \frac{(14.5)^2}{60} = 3.5 \Omega \tag{40}$$

The formula presented in [16] was used to calculate the value of input capacitor C_1 ,

$$C_1 = \frac{V_o \cdot D}{R \cdot f_{sw} \cdot \Delta V_{c1}} = \frac{14.5 \cdot 0.86}{48 \cdot 8 \cdot 10^3 \cdot 1.41} = 223 \mu F \tag{41}$$

An aluminum electrolytic capacitor with low equivalent series resistance (ESR) type is required. The value of the output capacitor (C_2) is calculated using the output voltage ripple equation (the same as that of buck converter) [27].

$$\frac{\Delta V_o}{V_o} = \frac{1 - D}{8 \cdot L_2 \cdot C_2 \cdot f_{sw}^2} \tag{42}$$

Solving equation 42 for C_2 gives equation 43.

$$C_2 = \frac{1 - D}{8 \cdot \frac{\Delta V_o}{V_o} \cdot L_2 \cdot f_{sw}^2} = \frac{1 - 0.86}{8 \cdot 0.05 \cdot 990 \cdot 10^{-6} \cdot (8 \cdot 10^3)^2} = 470 \mu F \tag{43}$$

NB; for both capacitors, their voltage capacities are 200V and have above 10A current rating.

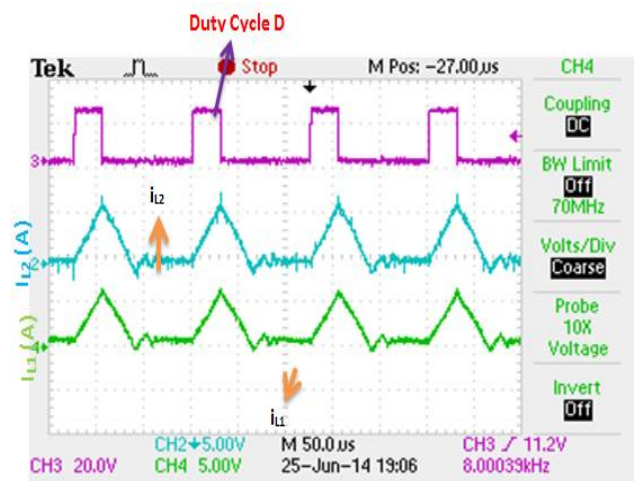


Figure 7: Laboratory results for the two inductors in Cuk converter in DICM

2.5. Incremental Conductance Method of MPPT

This method was first presented in [28] and it is based on the observation that in the MPP, the following condition occurs:

$$\frac{dp}{dV} = \frac{d(V \cdot I)}{dV} = 0 \tag{44}$$

where dP is the derivative of P , dV is the derivative of V and $d(VI)$ is the derivative of power (VI).

By accounting for the dependence of the PV current on the voltage, it is possible to express such a condition as follows [29]

$$I + V \frac{dI}{dV} \tag{45}$$

where I is the system current and dI is the current derivative.

So that the validity of condition in (44) is equivalent to

$$\frac{dI}{dV} = -\frac{I}{V} \tag{46}$$

By these conditions, it means that at the MPP, the absolute value of the conductance must be equal to the absolute value of the incremental conductance. Condition in equation (46) is verified through a repeated measure of the conductance at two different, but closed values of the PV voltages. To this effect, the method requires the application of a repeated perturbation of the voltage which may be as a result of varying environmental conditions; until this condition is meant:

$$\frac{I_k}{V_k} = -\frac{I_k - I_{k-1}}{V_k - V_{k-1}} \tag{47}$$

where the subscripts k and $k-1$ refer to two consecutive samples of the PV voltage and current values as captured by PIC16F877 microcontroller.

The evaluation of equation (47) can be useful in order to understand on which side of the P-V curve with respect to the MPP that the actual operating point lies.

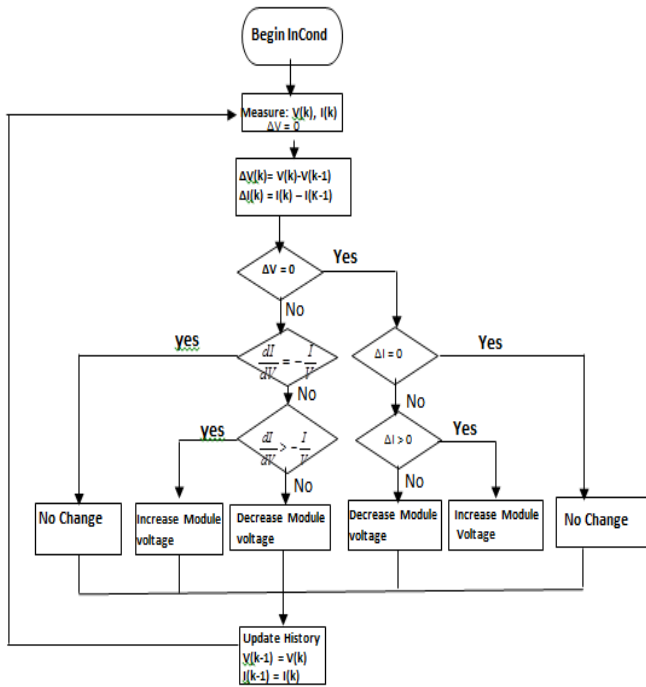


Figure 8: Flowchart of the incremental conductance algorithm

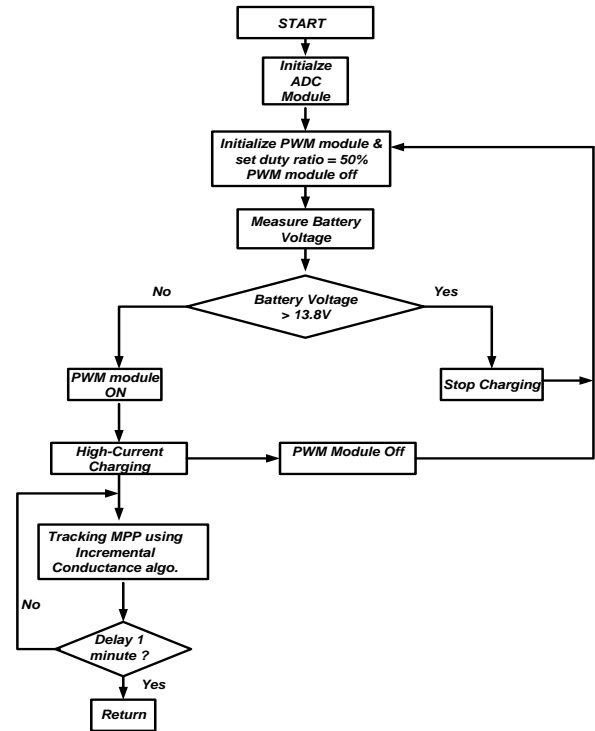


Figure 9: Program Flow Chart

Combining equations(45) and (46) we get;

$$\frac{I}{V} \cdot \frac{dP}{dV} = \frac{I}{V} + I \frac{dV}{dV} + \frac{dI}{dV} = G + dG \quad (48)$$

Where G is the conductance and dG is the incremental conductance. That shows that, on the left side of the P-V curve with respect to the MPP, $dP/dV > 0$. This means that $G + dG > 0$. Hence, if the conductance is greater than the absolute value of the incremental conductance, then the operating point is on the left side of the MPP, so the voltage must be increased in order to move closer to the MPP. By so doing the duty cycle of the Cuk converter operating in DICM will then increase and vice versa.

The new voltage at which condition (46) must be tested is evaluated according to the following iterative formula;

$$V_{PV}^{k+1} = V_{PV}^k + \text{sign}(G + dG) \cdot \Delta V \quad (48)$$

Where ΔV is the voltage step chosen for the perturbative phase during which the MPP is searched [30]. The flowchart for incremental conductance is as shown in Figure 8.

5. Experimental Setup for DICM Cuk Converter

The design of the on-board software control was done using PIC16F887 microcontroller. The PIC16F887 microcontroller operating at the speed of 5 MHz is used to carry out the algorithm. This gives executive clock cycle of 0.2μ second. The program is written in Assembly Language and compiled using Top Win programmer. The program flow chart is shown in Figure 9. The program starts by initializing the A/D module and setting D/A (PWM) module and at duty ratio at 50%, around which

the MPP can be found. The prototype is made up of different sections which include the control unit (consisting of PIC16F877, the written code and the peripheral circuits), power supply unit, the gate driver unit, the battery charging unit, the buffer/isolator unit and the feedback unit. Figure 10 depicts the laboratory prototype of the work (a maximum power point tracking scheme for 1 kW stand-alone solar energy based power supply). This Figure 10 shows the indoor setup of the prototype using oscilloscope.

3. RESULT AND ANALYSIS

Figures 11and 12 show the effect of varying radiation at constant temperature and varying temperature at varying radiation respectively, which results from the modeling of PV system carried out in this section. With the increase of solar radiation, the short-circuit current of the PV generator module increases, and the maximum power output increases as well. The reason is that the open-circuit voltage is logarithmically dependent on the solar irradiance, yet the short-circuit current is directly proportional to the radiant intensity. As a result, the global PV system efficiency increases in this case Based on the findings of [31], that tracking the maximum value of the load current or voltage implies operating of the PV system at its MPP. The controller simplicity translates into a reduction in the hardware involved, in terms of sensors, and in a MPPT algorithm that does not require the multiplication needed for calculation of the PV power. Based on this, only output voltage of the

prototype was monitored and presented in this research work.

The MPPT is at the positive side trying to locate the peak value so as the duty cycle increases from 0.17 to 0.32 the output voltage also increases from -5.0V to -10.0V. By so doing, the prototype obeys perfectly the equations developed in equations(43) to (47). The duty cycle has increased from its previous value of 0.17 to 0.32, at this point the input voltage decreased from 17 V to 12 V as seen in Figure 13. Inspecting Figures 14, one will observe

that when the duty cycle is 0.72, the input voltage is 12.0 V while the output voltage is - 18.0 V.

Similarly, when the duty cycle changes to 0.84 there was no change in the output voltage even though the input voltage decreases to 10V indicating that the MPP of the solar panel at the specified environmental conditions has reached as seen in Figure 15. Similarly, there are two prominent factors that affect seriously the performance of any PV panel. These include sun irradiance and ambient temperature. The two are equally investigated and the results are shown in Figures 17 to 19.



Figure 10 Laboratory Setup

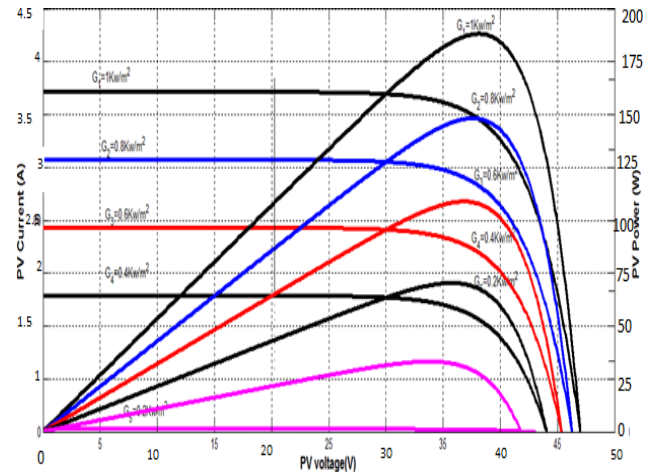


Figure 11: I-V and P-V characteristic at varying insolation

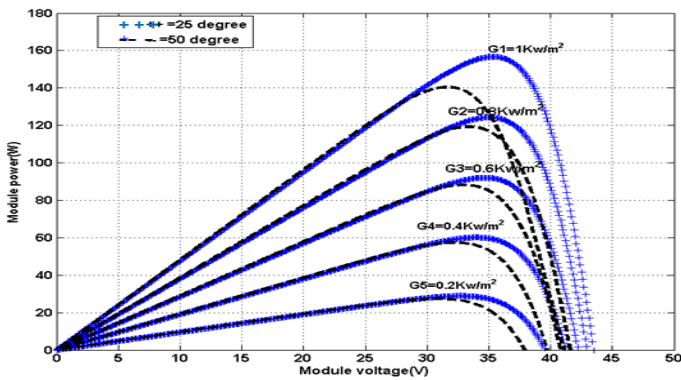


Figure 12: Effect of varying temp on P-V Characteristic Power

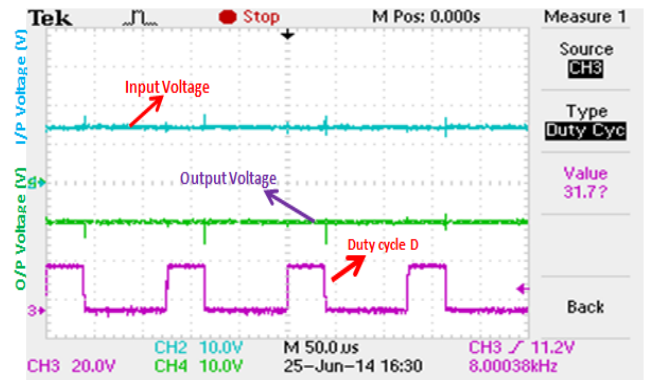


Figure 13: Output /Input Voltage at D = 0.32 @ 8kHz frequency

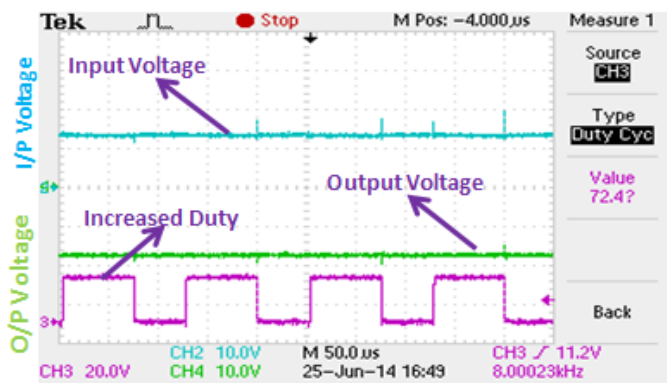


Figure 14: Output /Input Voltage at D= 0.72 @ 8 kHz frequency

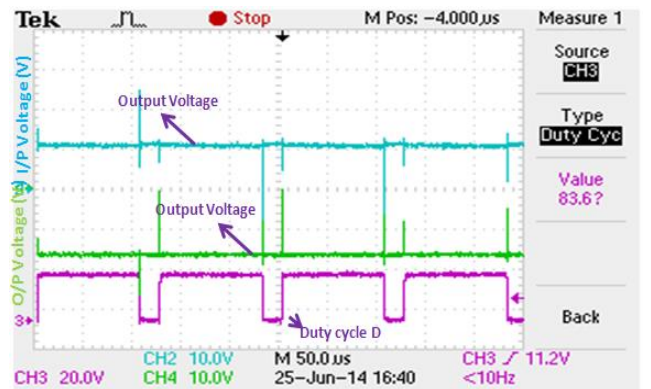


Figure 15 Output /Input Voltage at D= 0.84 @ 8 kHz frequency

There was a transient that lasted for 0.1 sec but in this case the transient was not as severe as in P&O method of MPPT as depicted in Figure 16. At the steady state, the output power is 1.15kW. But Figure 17 shows how temperature affects PV power. At ambient temperature of 25 ° C at constant solar insolation, the PV power output was 200W/m², but as the temperature increases to 50 ° C the power reduced to 149W/m² with a lot of heat produced around the panel.

That was so since the panel converts only one out of many rays of light spectrum to direct current while all other rays generate heat around the panel. If in nature the temperature can reach up to 75 °C, then the power will be around 26W/m².

Figure 18 shows how the power output of PV system vary with varying insolation. At 1kW/m² of the irradiation at constant temperature the power output is 200W but when the irradiance changes to 800W/m² the corresponding power was 160W while at 600W/m² irradiance, its power was 119W still at constant temperature. Figure 19 demonstrates the effect of maximum power point controller in PV system generation. The figure was generated using InCond method of MPPT on Cuk converter operating in DIC mode. The MPPT was enabled at 0.53 seconds, the power output performance increased by 17.65%.

4. CONCLUSION

Efforts are being made to promote green electric generation which is conducive to the preservation and enhancement of healthy environmental conditions. Therefore, the main objective of this research was on a technique for efficiently extracting the maximum output power from the solar panel. A PWM dc – dc Cúk converter operating in discontinuous inductor current was used to match with the output resistance of the panel. By adjusting the duty cycle of the Cúk converter, the MPP can be located. The method used in extracting the MPP in this work was incremental conductance method. The PV models were analyzed and from the analysis carried out, PV simulator as it often called was modeled in MATLAB /SIMULINK software. The Cúk converter was also modeled in MATLAB/SIMULINK environment and PV simulator was used to power it for simulation work. The result of varying meteorological conditions investigated confirm the theoretical analysis. The control logic for the experimental MPPT algorithm was implemented using PIC16F887 microcontroller which was aimed at reducing the components and improving the efficiency of the system.

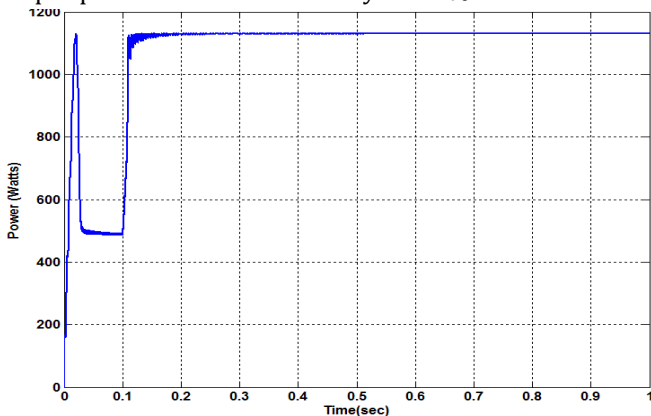


Figure 16: Cúk DICM Output Power (P_{out})

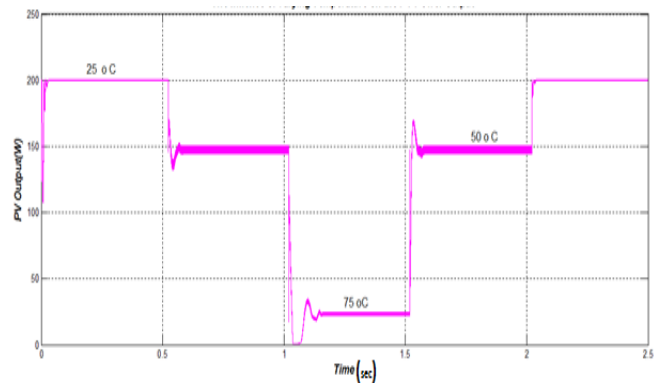


Figure 17: PV Power Output at varying Temperature at constant insolation

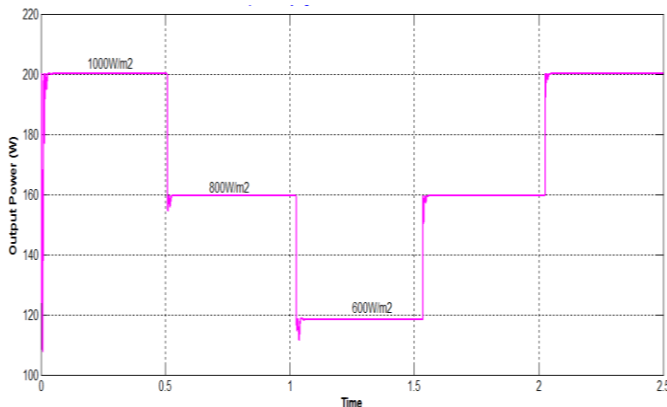


Figure 18: PV Power Output at varying insolation at constant temperature

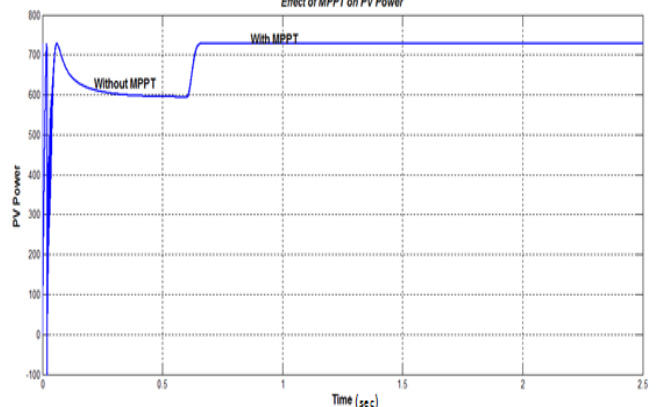


Figure 19: Demonstration of MPPT Power enhancement on PV Panel

Finally, the laboratory prototype of a 1kW, 230V, 50Hz stand-alone solar base power supply with the incremental conductance scheme of MPPT operating with Cúk converter in discontinuous inductor current mode was successfully built and tested. The findings from the prototype disclosed that there was 17.65% enhancement when compared with PV panel supplied without MPPT device. The output voltages at various duty cycles increased till the point of $\frac{dp}{dv} = 0$ as observed from theory. Similarly, all the step by step requirements needed for the installation and proper functioning of MPPT stand-alone solar energy based power supply are presented.

5. REFERENCES

- [1] Leon Freris, David Infield, "Renewable Energy in Power Systems", A John Wiley & Sons, Ltd, Publication, First edition, The Atrium, Southern Gate, Chichester, West Sussex, PO19, 8SQ, United Kingdom, 2008.
- [2] VijayaVenkataRaman, S., S. Iniyan, and R. Goic. "A Review of Climate Change, Mitigation and Adaptation", *Renewable and Sustainable Energy Reviews* 16 (1): 878-897, 2012.
- [3] Federico M. Butera, "Zero-energy buildings: the challenges", *Advances in Building Energy Research, Taylor & Francis*, Vol. 7, No. 1, 51-65, 2013
- [4] Marino Coppola, Fabio Di Napoli, PierluigiGuerrero, Adolfo Dannier, Diego Iannuzzi, Santolo, Daliento, and Andrea Del Pizzo, "Maximum Power Point Tracking Algorithm forGrid-tied Photovoltaic Cascaded H-bridge Inverter" *Electric Power Components and Systems*, 43(8-10):951-963, 2015.
- [5] Salas, V., Olias, E., Barrado, A., and Lazaro, A., "Review of the maximum power point tracking algorithms for stand-alone photovoltaic systems," *Sol. Energy Mat. Sol. Cells*, Vol. 90, No.11, pp. 1555-1578, 2006.
- [6] Wai, R. J, Lin, C. Y, and Chang, Y. R, "Novel maximum-power extraction algorithm for PMSG wind generation system," *IETElectr. Power Appl.*, Vol. 1, No. 2, pp. 275-283, 2007.
- [7] Nicola F. E., Giovanni P., Giovanni S., and Massino V., "Optimization of Perturb and Observe Maximum Power point tracking Method", *IEEE Trans Power Electronics*. vol. 20, no. 4, July 2005
- [8] Sofia Lalouni, Djamila Rekioua, Kassaldjdarene & Abdelmounaim Tounzi, "Maximum Power Point Tracking Based Hybrid Hill-climb Search Method Applied to Wind Energy Conversion System *Electric Power Components and Systems*, 43(8-10):1028-1038, 2015
- [9] Mohmmad A. S . M., Hooman D., and Ewald F. F, "Theoretical and Experimental Analyses of Photovoltaic Systems with Voltage- and Current-Based Maximum Power Point Tracking", *IEEE Transaction on Energy Conversion*. vol.17, no 4. Dec.2002.
- [10] Schoeman]. J. and Van Wyk J. D., "A simplified maximal power controller for terrestrial photovoltaic panel arrays," *13th Annual IEEE Power Electronics. Specialists Conference*, pp. 361-367, 1982.
- [11] Veerachary M; Senjyu, T. and Uezato, K; "Neural-network-based maximum- Power point tracking of coupled-inductor interleaved-boost converter-supplied PV system using fuzzy controller," *IEEE Trans. Industrial Electronics*, vol. 50, Pp. 749-758, Aug. 2003
- [12] Feng W, Xinke W, Fred C. Lee, Z .W, Pengju W, Pengju K and Fand Zhuo, "Analysis of Unified Output MPPT Control in Subpanel PV Converter system", *IEEE Transaction on Power Electronics*, vol. 29, no.3, pp. 1275 -1284, March 2014,
- [13] S. Busso and P. Mattavelli, "Digital Control in Power Electronics". San Rafael, CA: Morgan & Claypool Publishers, 2006.
- [14] S. Chun and A. Kwasinski, "Analysis of Classical Root-Finding Methods Applied to Digital Maximum Power Point Tracking for Sustainable Photovoltaic Energy Generation". *IEEE Transaction on Power Electronics*, vol. 26, no. 12, pp.3730 -3743, Dec. 2011
- [15] J.W. Kimball and P. T. Krein, "Discrete-time ripple correlation control for maximum power point tracking," *IEEE Trans. Power Electron.*, vol. 23, no. 5, pp. 2353-2362, Sep. 2008.
- [16] F. Liu, S. Duan, F. Liu, B. Liu, and Y. Kang, "A variable step size INC MPPT method for PV systems," *IEEE Transaction on Industrial Electron.*, vol. 55, no. 7, pp. 2622-2008, Jul. 2008.
- [17] R.-Y. Kim, J.-S. Lai, B. York, and A. Koran, "Analysis and design of maximum power point tracking scheme for thermoelectric battery energy storage system," *IEEE Trans. Ind. Electron.*, vol. 56, no. 9, pp. 3709-3716, Sep. 2009.
- [18] Moacyr Aureliano Gomes de Brito, Luigi Galotto, Jr., Leonardo Poltronieri Sampaio, Guilherme de Azevedo e Melo, and Carlos Alberto Canesin, "Evaluation of the main MPPT techniques for Photovoltaic applications", *IEEE Transactions on Industrial Electronics*, vol. 60, no. 3, March 2013
- [19] Azadeh Safari and Saad Mekhilef, "Simulation and hardware implementation of incremental

- conductance MPPT with direct control method using Cuk converter", *IEEE Transactions on Industrial Electronics*, vol. 58, no. 4, April 2011
- [20] D. B. N. Nnadi, "Environmental/Climatic Effect on Stand-Alone Solar Energy Supply Performance for Sustainable Energy" *Nigerian Journal of Technology (NIJOTECH)*. vol. 31, no. 1, pp. 79-88, March, 2012.
- [21] Masters, G. M. "*Renewable and Efficient Electric Power Systems*", John Wiley & Sons Ltd, 2004
- [22] Hart, G. W. Branz, H. M and Cox, C. H, "Experimental tests of open loop maximum- Power point tracking techniques," *Solar Cells*, vol. 13, pp. 185-195, 1984.
- [23] Tse K. K.; Ho M. T.; Henry S. H.; Chung; Ron Hui S. Y. "A novel MPPT for PV panels using switching frequency modulation", *IEEE Transaction on Power Electronics* 17, (2002)
- [24] Henry S.H Chung, Tse, K. K, S. Y. Ron Hui, C. M. Mok, and M. T. Ho.: A novel MPPT technique for solar panels using a SEPIC or Ćuk Converter. *IEEE Transaction Power Electronics*, 18, 717 - 724 (2003)
- [25] Lin B, and Lee, Y, "Power-factor correction using Cuk converters in discontinuous- capacitor voltage mode operation," *IEEE Transaction on Industrial Electronics*, vol. 44, pp. 648- 653, Oct. 1997.
- [26] Maksimovic D. and Cuk, S, "A unified analysis of PWM converters in discontinuous modes", *IEEE Transaction on Power Electronics*, vol. 6, pp. 476-490, Mar. 1991.
- [27] Hart, D. W. "*Introduction to Power Electronics*" Prentice Hall Inc., 1996.
- [28] Akihiro Oi, "Design and Simulation of Photovoltaic Water Pumping System", A Thesis Presented to the Faculty of California Polytechnic State University, San Luis Obispo, Sept. 2005.
- [29] K.H. Hussein, I. Muta, T. Hoshino and M. Osakada, "Maximum photovoltaic power Tracking: An algorithm for rapidly changing atmospheric conditions", *IEE Proceedings of Generation, Transmission and Distribution*, 142(1): 59-64, 1995
- [30] Nicola Femia, Giovanni Petrone, Giovanni Spagnuolo, & Massimo Vitelli, "*Power Electronics and Control Techniques for Maximum Energy Harvesting in Photovoltaic Systems*", CRC Press, Taylor & Francis Group, 6000 Broken Sound Parkway NW, Suite 300, 2013
- [31] D. Shmilovitz, "Control of Photovoltaic maximum power point tracker via output parameters", *IEEE Proceedings of Electric Power Applications*, 152(2):239-248, 2005.